

Quenched approximation in the quark model

Paul Geiger and Nathan Isgur

Department of Physics, University of Toronto, Toronto, Canada M5S 1A7

(Received 7 September 1989)

We present a model calculation of some effects of virtual $q\bar{q}$ pairs in mesons. Specifically, using a model for pair creation that has previously been shown to give a good description of strong meson decays, we calculate the energy shift of a static quark-antiquark pair due to the presence of virtual quark-antiquark pairs. The shift is large and approximately proportional to the distance between the static sources. The linearity of the correction suggests that pair-creation effects can be absorbed into a renormalization of the mesonic string tension. However, this masking can only be approximate, as we show by considering the dependence of the energy shift on the spin state of the sources. We conclude by pointing out the relevance of our results to the “ N/ρ ” problem encountered in lattice QCD calculations.

I. INTRODUCTION

Recent advances in computing power and new sophisticated algorithms have made it possible to undertake lattice studies of full (“unquenched”) QCD, wherein the usual approximation of ignoring dynamical quarks is not made. These calculations indicate¹ that the dynamical quarks cause large (negative) shifts both in the quenched hadron masses and in the quenched interquark potential. It is often claimed that these large shifts can be absorbed into a renormalization of the lattice coupling constant. However, the reliability of these claims is compromised by the facts that only a few, low-lying hadron masses have been computed, and that unquenched calculations can, at present, be performed only on quite small lattices, with unphysically large quark masses.

Several model calculations of the effects of (virtual) dynamical quarks in hadrons have also been made.² They generally give results that are qualitatively similar to the lattice results; i.e., they predict large negative shifts in the interquark potential and in hadron masses. However, none of these models is entirely satisfactory: they all treat the creation of the virtual quark pairs in an *ad hoc* or schematic way.

In this paper we present a new model calculation of the effects of dynamical quarks in mesonic systems. We consider a state consisting of a static $Q\bar{Q}$ pair joined by a chromoelectric flux tube, and we determine how the energy of this state changes when it is allowed to mix with $Q\bar{q}q\bar{Q}$ states. The operator that produces the mixing is taken from a recent model of meson decays,³ so that our treatment is well grounded phenomenologically. We find a large shift in the $Q\bar{Q}$ potential. We then go on to calculate, in the same phenomenological picture, the *differential* energy shift between a spin-triplet $Q\bar{Q}$ pair and a spin-singlet $Q\bar{Q}$ pair. This differential shift turns out to be substantial, indicating that the effects of dynamical fermions cannot all be absorbed into a change in a single coupling constant. Finally, we show that, as the “bare” mass of a particular resonance is varied, the crossing of a decay threshold can cause its mass shift from vir-

tual pair creation to change abruptly. We comment on the ramifications of this observation for the “ N/ρ ” problem of lattice calculations.

II. A MODEL FOR PAIR CREATION IN MESONS

Our model for describing virtual pair creation in mesonic systems is essentially the same as the one used in the flux-tube model⁴ to describe meson decays via real pair creation.³ We therefore begin with a brief account of the flux-tube model, with an emphasis on those features that are particularly relevant to the present calculation.

The flux-tube model is based on the strong-coupling limit of Hamiltonian lattice QCD (Ref. 5). When QCD is formulated on a lattice, in the limit where the lattice spacing a and therefore the coupling constant g approach infinity, the eigenstates of QCD become quite simple: they consist of “frozen” configurations of quarks and antiquarks on the lattice sites, joined by flux lines which live on the links between sites. Some examples of these strong-coupling eigenstates are shown in Fig. 1.

When the lattice spacing is finite, two new terms appear in the QCD Hamiltonian, causing these strong-coupling eigenstates to mix. The first of these terms is

$$\sum_{\text{plaquettes}} \text{Tr}[2 - (U_{l_1} U_{l_2} U_{l_3} U_{l_4} + \text{H.c.})],$$

where U_{l_i} is an operator that creates a unit of 3-flux on link i . The product of U 's is taken around an elementary square or “plaquette” on the lattice, so this first operator creates plaquette-sized loops of 3-flux. It is responsible for flux-tube hopping, flux-tube rearrangement, and other effects, as illustrated in Fig. 2. The second operator that becomes important at finite lattice spacings is

$$\sum_{\text{links } l_{ji}} q_j^\dagger U_{ji} \alpha_{ji} q_i,$$

where q_i is the quark field operator at site i , and α_{ji} is the Dirac matrix in the direction of the link l_{ji} . This operator creates a quark and antiquark at neighboring lattice

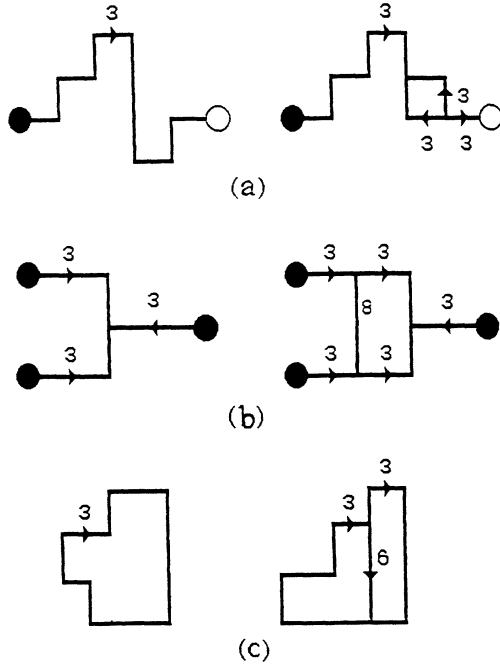


FIG. 1. (a) Some strong-coupling meson states; (b) some strong-coupling baryon states; (c) some strong-coupling pure glue states.

sites, connected by a line of 3-flux. It is responsible, as Fig. 3 indicates, for quark-hopping, flux-tube breaking, and other effects.

The various actions of these two operators on strong-coupling eigenstates can be divided into two categories: those, like flux-tube breaking and flux-tube rearrangement, which change the topology⁶ of a state, and those,

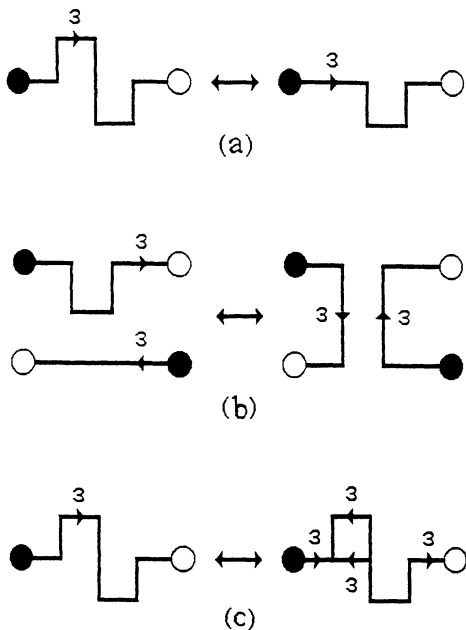


FIG. 2. Some effects of $\text{Tr}(U_1 U_2 U_3 U_4 + \text{H.c.})$: (a) flux-tube hopping; (b) flux-tube rearrangement; (c) "bubble formation."

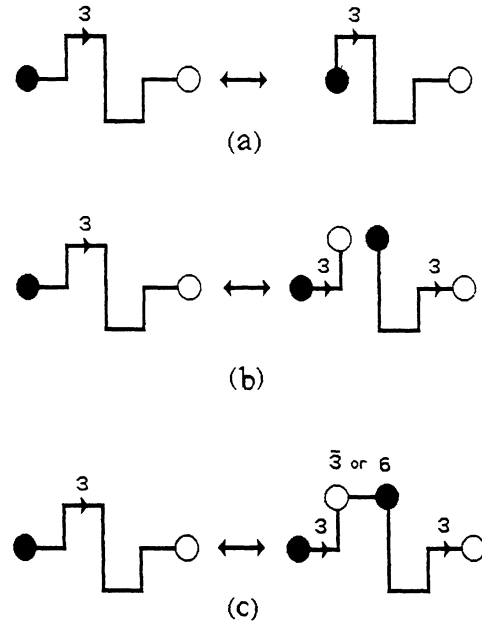


FIG. 3. Some effects of $q^\dagger U a q$: (a) quark hopping; (b) flux-tube breaking/pair creation; (c) $q\bar{q}$ "seeding."

like quark and flux-tube hopping, which do not. The strategy adopted in the flux-tube model is to treat the latter effects exactly, by organizing the strong-coupling eigenstates into blocks of fixed topology and diagonalizing within each block, and then to treat the topological mixing between blocks perturbatively.

We are particularly interested in how mesons are described in the flux-tube model. Consider fixed Q and \bar{Q} sources, separated by a distance $r \gg b^{-1/2}$ (where b is the QCD string tension: $b \approx 0.18 \text{ GeV}^2$), and connected by a line of 3-flux. The long-distance properties of this $Q\bar{Q}$ system ought to be well described on a lattice with spacing $a \sim b^{-1/2}$. On such a lattice one is not too far from the strong-coupling limit, and it seems reasonable to neglect topological mixing and consider only the flux-tube hopping effects, which allow the string to "vibrate." Thus, in this approximation, the energy levels $V^n(r)$ of the $Q\bar{Q}$ system are simply the energies of a (discrete) vibrating quantum string. To recover the usual quark model for mesons, one identifies these levels as a set of *adiabatic potentials* in which the quark and antiquark move. The lowest-energy surface $V^0(r)$ corresponds to ordinary mesons, while the excited surfaces correspond to vibrational hybrids. In Ref. 4 it was shown that the ground-state energy of the latticized, vibrating, quantum string is proportional to the length of the string (in the limit of a very long string). Once the constant of proportionality is identified as the physical string tension b the adiabatic potential $V^0(r) = br$ gives, in the context of the quark potential model, a reasonable account of the gross level structure of meson spectroscopy.

In this paper we will study the way in which this lowest-order picture of mesons, which in its neglect of the effect of dynamical $q\bar{q}$ pairs corresponds to the quenched

approximation of Euclidean lattice QCD, changes when the effects of the pair-creation operator $q^\dagger U a q$ are taken into account. Specifically, in Sec. III we will consider a system consisting of two fixed Q and \bar{Q} sources joined by a string in its vibrational ground state. We will use perturbation theory to calculate, as a function of the $Q\bar{Q}$ separation r , the energy shift $\Delta E(r)$ produced by the interaction responsible for meson decay, in the approximation that spin-dependent forces between the quarks are negligible. We will see that $\Delta E(r)$ is approximately linear in r , so that $\Delta b \equiv (d/dr)\Delta E(r)$ can be identified as the correction to the mesonic string tension. In Sec. IV we will include spin-dependent forces in our model and find that the value one obtains for Δb is sensitive to the spin state of the $Q\bar{Q}$ system, so that a simple renormalization of b cannot absorb all the effects of the virtual pairs.

III. SPIN-INDEPENDENT CALCULATION OF THE ENERGY SHIFT

We will calculate ΔE perturbatively in the strength of the pair-creation amplitude. [The treatment of pair-creation effects as weak corresponds both to the usual narrow-resonance approximation and to the large- N_c (N_c is the number of colors) limit. Nevertheless, as we will see below, this approximation may require further consideration.] Then ΔE can be separated into two parts: The first part, which we will call ΔE_{sb} , arises from the virtual breaking and rehealing of the mesonic string; the second part ΔE_{vac} , comes about because the pair-creation operator modifies not only our mesonic state, but the vacuum state as well, and we must subtract off the vacuum energy from our calculated meson energy.

Let us deal first with ΔE_{sb} . Our initial, unperturbed state is completely characterized by the positions of its fixed Q and \bar{Q} sources, whose relative coordinate \mathbf{r} we can take to be along the z axis. Recall that we are taking the string between these sources to be in its ground state. Also note that the sources are "spectators" throughout the calculation: their flavors and (for this first calculation) spins do not enter into the problem, so we do not need to specify them. The initial state can thus be denoted simply by $|\mathbf{r}\rangle$.

The operator $q^\dagger U a q$, when applied to this state, can break the string into two pieces, creating a quark q on the end of the \bar{Q} piece, and an antiquark \bar{q} on the end of the other piece. The resulting $\bar{Q}q\bar{q}Q$ state (see Fig. 4) may be labeled by the quantum numbers of two virtual mesons. We will use nonrelativistic wave functions for these

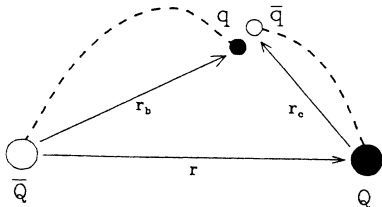


FIG. 4. Coordinates for string breaking.

mesons. This choice makes the calculation tractable, and it finds some justification in recent work⁷ on the "relativization" of the quark model, which indicates that relativistic effects in hadrons can to a large extent be absorbed into the parameters of the nonrelativistic quark model. Labeling the virtual mesons by the usual spectroscopic quantum numbers n, l, m , and s , we can write the intermediate states as $|n_b, l_b, m_b, s_b; n_c, l_c, m_c, s_c\rangle$; then the energy shift from string breaking is given by

$$\Delta E_{sb}(\mathbf{r}) = \sum_{\substack{n_b, l_b, m_b, s_b \\ n_c, l_c, m_c, s_c}} \frac{|\langle n_b, l_b, m_b, s_b; n_c, l_c, m_c, s_c | H_{sb} | \mathbf{r} \rangle|^2}{V^0(r) - E_{bc}}, \quad (1)$$

where H_{sb} is an effective string-breaking-pair-creation operator, to be constructed from the lattice operator $q^\dagger U a q$.

Before discussing H_{sb} , we have several comments to make concerning (1). First, the sum over intermediate states should properly include not only ordinary meson states, but hybrid (i.e., excited-string) meson states as well. However, we will later argue that such states make a relatively small contribution to ΔE_{sb} , so we have simply omitted them. Second, the statement that relativistic effects in hadrons can be absorbed into the parameters of the nonrelativistic quark model cannot be expected to hold for very highly excited hadrons. It is therefore fortunate that, for $r \lesssim 2$ fm, the major contributions to the sum (1) come from meson states with small n and l . (Typically, the terms in the series die off rapidly for $n, l \geq 5$.)

If the Q and \bar{Q} were not fixed in position, but rather were in some wave function $\Psi(\mathbf{r})$, then the effect of the pair-creation operator would be to allow this $Q\bar{Q}$ meson to decay into $Q\bar{q}$ and $q\bar{Q}$. Indeed, the authors of Ref. 3 used exactly this picture to calculate the amplitudes for the simple strong decay modes of all the low-lying mesons; that they obtained excellent correspondence with experiment supports the validity of the model. Let us therefore summarize their construction of the effective string-breaking operator H_{sb} , introducing a minor modification along the way.

To begin, observe that when the mesonic string is broken on the link between sites \mathbf{n} and $\mathbf{n} + \hat{\mathbf{e}}$, the newly formed quark pair is created with an effective operator

$$C_{\mathbf{n}, \hat{\mathbf{e}}} = \frac{3\gamma(\mathbf{n})}{a} \sum_q q^\dagger(\mathbf{n}) \vec{\alpha} \cdot \hat{\mathbf{e}} q(\mathbf{n} + \hat{\mathbf{e}}). \quad (2)$$

The factor $3\gamma(\mathbf{n})$ contains the amplitude for the newly broken string to be found in the wave functions of the final-state string pieces. Expanding $q(\mathbf{n} + \hat{\mathbf{e}}) \approx q(\mathbf{n}) + a\hat{\mathbf{e}} \cdot \nabla q(\mathbf{n})$ gives

$$C_{\mathbf{n}, \hat{\mathbf{e}}} = \frac{3\gamma(\mathbf{n})}{a} \sum_q q^\dagger(\mathbf{n}) \vec{\alpha} \cdot \hat{\mathbf{e}} q(\mathbf{n}) + 3\gamma(\mathbf{n}) \sum_q q^\dagger(\mathbf{n}) \vec{\alpha} \cdot \hat{\mathbf{e}} \hat{\mathbf{e}} \cdot \nabla q(\mathbf{n}). \quad (3)$$

At this point it is argued in Ref. 3 that one should average over $\hat{\mathbf{e}}$, since "roughening" at the scale a makes the piece of string that is cut out at this scale unoriented.

This gives

$$C_n = \gamma(\mathbf{n}) \sum_q q^\dagger(\mathbf{n}) \vec{\alpha} \cdot \vec{\nabla} q(\mathbf{n}). \quad (4)$$

C_n creates a $q\bar{q}$ pair in a 3P_0 state at the point \mathbf{n} .

We may write the string overlap function $\gamma(\mathbf{n})$ as $\gamma_{bc}^a(\mathbf{n})$ to remind ourselves that it depends on the state of the original string (string a), and on the states of the broken string pieces (strings b and c). As discussed in Ref. 3, all of these functions can be computed analytically in the limit where the string oscillations are small compared to the length of the string. Their explicit forms are messy and not very enlightening. However, the function $\gamma_{00}^0(\mathbf{n})$, which gives the amplitude for a ground-state string to break into two ground-state string pieces, is well approximated by $\gamma_0 e^{-(b/2)w_{\min}^2}$, where γ_0 is a constant, and w_{\min} is the shortest distance from the point \mathbf{n} to the line joining Q and \bar{Q} . The equipotentials of this function are cigar shaped (see Fig. 5), and string breaking thus occurs inside a ‘‘cigar’’ of volume $V \sim \pi r/b$. The factor γ_0 may be interpreted as an elementary pair-creation amplitude, and it can be determined by calculating decay rates in the string-breaking model and fitting to experiment (see the Appendix for details of this procedure and for results).

The analytic calculation of $\gamma_{00}^0(\mathbf{n})$ shows (again in the small oscillations limit) that, when a ground-state string breaks, the probability for the broken pieces to be in their ground states is close to unity for lattice spacings of the size we are considering: it varies between approximately 0.8 and 0.9 for a 1–2-fm-long string, with a in the range

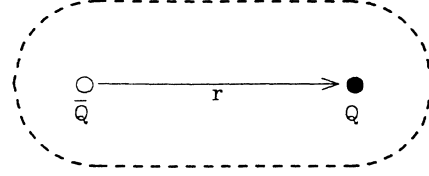


FIG. 5. A contour of $\gamma_{00}^0(\mathbf{r})$.

0.1 to 0.2 fm. Thus, there is very little probability for the string to break into excited string pieces. This is the main justification for ignoring hybrid mesons in the sum (1). In addition, hybrid mesons typically have larger masses than ordinary mesons, so their effect on ΔE_{sb} is further diminished by the energy denominator in (1).

We cannot use (4) as it stands in our calculation of ΔE_{sb} , for if we use

$$H_{sb} = \int d^3r C_r = \int d^3r \gamma_{00}^0(\mathbf{r}) q^\dagger(\mathbf{r}) \vec{\alpha} \cdot \vec{\nabla} q(\mathbf{r}) \quad (5)$$

in (1) we find by explicit calculation that the sum does not converge. [We have not been able to prove this in general, but we can show analytically that when the string length is zero, and the meson wave functions are taken to be harmonic-oscillator wave functions, Eq. (1) gives an infinite result.] The problem can be traced to the point-like nature of the effective pair-creation operator C_r . Because the quarks being created are constituent quarks with some effective size, we should make the replacement

$$C_r \rightarrow \tilde{C}_r = \left[\frac{3}{8\pi r_q^2} \right]^{3/2} \int d^3u e^{-(3u^2/8r_q^2)} \gamma_{00}^0(\mathbf{r}) q^\dagger \left[\mathbf{r} + \frac{\mathbf{u}}{2} \right] \vec{\alpha} \cdot \vec{\nabla} q \left[\mathbf{r} - \frac{\mathbf{u}}{2} \right], \quad (6)$$

where r_q is the ‘‘radius’’ of a constituent quark. Of course, this operator still creates a 3P_0 pair, and it reduces to C_r when r_q goes to zero.

When we reproduce the meson decay calculations of Ref. 3 using \tilde{C}_r in place of C_r , we find that the quark form factor suppresses those decays in which the final-state mesons have a large relative momentum. Thus, by comparing the calculated rates for such decays, as a function of r_q , to the experimental rates, we can set an upper bound on r_q , and thereby a lower bound on the magnitude of ΔE_{sb} . This is done in the Appendix, where we conclude that r_q is almost certainly less than 0.3 fm.

With this information we may calculate $\Delta E_{sb}(r)$. For each $q\bar{q}$ flavor, Eq. (1) can be written in terms of the wave functions of the virtual mesons as

$$\Delta E_{sb}(r) = 2 \left[\frac{3}{8\pi r_q^2} \right]^3 \sum_{\substack{n_b l_b m_b \\ n_c l_c m_c}} \frac{\left| \int d^3u d^3v e^{-(3u^2/8r_q^2)} \gamma_{00}^0(\mathbf{v}) \psi_b^*(\mathbf{v} + \frac{1}{2}\mathbf{u} + \frac{1}{2}r\hat{\mathbf{z}}) (\vec{\nabla}_c - \vec{\nabla}_b) \psi_c^*(\mathbf{v} - \frac{1}{2}\mathbf{u} - \frac{1}{2}r\hat{\mathbf{z}}) \right|^2}{V^0(r) - E_{bc}}, \quad (7)$$

where $\psi_b \equiv \psi_{n_b l_b m_b}$, and similarly for ψ_c . To arrive at this expression, we have performed the summations over the meson spins s_b and s_c . These sums can be done exactly since, in this first calculation, we are using a spin-independent potential model (see below) to obtain the wave functions ψ_b and ψ_c ; hence, the energy denominator in (1) is independent of s_b and s_c .

Computing ΔE_{sb} is challenging, as the number of terms in the sum is enormous, and each term is an in-

tegral which must be calculated numerically. In the six-dimensional integral over \mathbf{u} and \mathbf{v} , two of the integrations can be done analytically, thanks to the cylindrical symmetry of the problem. When these integrations are performed one finds that $m_b + m_c$ is constrained to be 0, +1, or -1. The remaining four-dimensional integrals contain products of spherical harmonics centered at different points, and they cannot be done analytically. This presents a problem because, in order to see very good

TABLE I. ΔE_{sb} (in GeV) as a function of the $Q\bar{Q}$ separation r , for various values of the quark mass m_q . The bottom row includes the contributions from *two* flavors of mass 0.33 GeV. The quark radius r_q was taken to be 0.30 fm.

m_q (GeV) \ r	0.0 fm	0.2 fm	0.6 fm	1.0 fm	1.4 fm	1.9 fm
0.33	-0.23	-0.30	-0.45	-0.63	-0.82	-1.08
0.55	-0.25	-0.33	-0.50	-0.70	-0.90	-1.12
1.8	-0.16	-0.21	-0.30	-0.39	-0.49	-0.62
5.2	-0.063	-0.078	-0.11	-0.14	-0.18	-0.24
Total	-0.92	-1.20	-1.81	-2.48	-3.21	-4.13

convergence of the series in (7), we typically need to sum up to $n_b \approx n_c \approx l_b \approx l_c \approx 10$ (although, as we have said, the major contribution to ΔE_{sb} comes from terms with $n_b, n_c, l_b, l_c \leq 5$), and this entails calculating approximately 300 000 integrals. However, the integrations in (4) are simple to perform analytically if the wave functions ψ_b and ψ_c are taken to be harmonic-oscillator wave functions, written in cylindrical coordinates. We therefore expanded ψ_b and ψ_c in a basis of such functions, as

$$|\psi_{nlm}\rangle = \sum_{Nn_z n'} |\chi_{Nn_z m}\rangle \langle \chi_{Nn_z m} | \chi_{n'lm}\rangle \langle \chi_{n'lm} | \psi_{nlm}\rangle, \quad (8)$$

where $|\chi_{Nn_z m}\rangle$ is a spherical harmonic oscillator (SHO) eigenfunction with ‘‘cylindrical’’ quantum numbers, and $|\chi_{n'lm}\rangle$ is an SHO eigenfunction with ‘‘spherical’’ quantum numbers. The overlaps $\langle \chi_{n'lm} | \psi_{nlm}\rangle$ may be calculated by diagonalizing the potential-model Hamiltonian in the $|\chi_{n'lm}\rangle$ basis, and the overlaps $\langle \chi_{Nn_z m} | \chi_{n'lm}\rangle$ are easily calculated analytically. We truncate the sum in (8) at the point where ΔE_{sb} becomes insensitive to the inclusion of higher terms.

Our results for ΔE_{sb} are shown in Tables I and II. Table I lists values for $r_q = 0.3$ fm; these values represent a lower bound on the magnitude of ΔE_{sb} (as discussed in the Appendix). The entries in Table II were calculated using $r_q = 0.25$ fm. They represent a more likely lower bound, and also serve to show how rapidly ΔE_{sb} increases as the constituent quark size decreases. We have performed the calculation for $u, d, s, c,$ and b quarks, with constituent masses of $m_u = m_d = 0.33$ GeV, $m_s = 0.55$ GeV, $m_c = 1.8$ GeV, and $m_b = 5.2$ GeV. The interquark potential was taken to be $V(r) = br + c$, with $b = 0.18$ GeV² and $c = -0.84$ GeV. (Our neglect of the usual Coulombic term in the potential is an approximation which is in line with our coarse-grained model of

mesons; the inclusion of such a short-distance effect would significantly influence the energies and wave functions of only the lowest-lying meson states.) Note the substantial contribution from $c\bar{c}$ and $b\bar{b}$ pairs. Note also that Eq. (7) has a sparse set of poles as a function of r . These poles correspond to degeneracies between the unbroken- and broken-string states. They are not a problem in practice, since they are artifacts of the use of lowest-order perturbation theory which become, when treated more exactly, small (~ 100 MeV) ripples on the function $\Delta E(r)$. The values of r appearing in Tables I and II are far from these poles, and so a smooth curve that interpolates between them will correspond to a definition of the string tension in the presence of dynamical pairs in which these ripples are averaged out.

We now turn to a calculation of ΔE_{vac} , which is the shift in the vacuum energy that is brought about by the creation of virtual $q\bar{q}$ pairs. (We will see that this calculation is subject to very large uncertainties; however, since ΔE_{vac} is an essential contributor to ΔE , we must at least attempt an estimate of it for completeness.) When applied to the vacuum state, H_{sb} will create a virtual 0^{++} meson. Since the vacuum energy shift from hybrid mesons is suppressed relative to that from normal mesons by the higher masses of the former, we stipulate, in accord with our previous neglect of hybrids, that H_{sb} should create only normal 0^{++} mesons, i.e., 3P_0 mesons. This leads to the result

$$\Delta E_{vac} = - \sum_n \int d^3P \frac{|\langle \mathbf{P}; n {}^3P_0 | H_{sb} | 0 \rangle|^2}{E_n(\mathbf{P})}, \quad (9)$$

where n is the principal quantum number of the 3P_0 meson, and \mathbf{P} is its center-of-mass momentum. We take H_{sb} to be given by (3), with the string overlap factor γ_{00}^0 removed. Then for each quark flavor we have for the vacuum energy shift per unit volume

TABLE II. Legend as for Table I, except that $r_q = 0.25$ fm.

m_q (GeV) \ r	0.0 fm	0.2 fm	0.6 fm	1.0 fm	1.4 fm	1.9 fm
0.33	-0.45	-0.60	-0.89	-1.21	-1.56	-2.01
0.55	-0.56	-0.72	-1.09	-1.47	-1.88	-2.37
1.8	-0.41	-0.52	-0.76	-1.00	-1.24	-1.55
5.2	-0.17	-0.21	-0.29	-0.38	-0.47	-0.58
Total	-2.04	-2.65	-3.92	-5.27	-6.71	-8.52

$$\Delta \mathcal{E}_{\text{vac}} = -(\gamma_0^{\text{vac}})^2 \left[\frac{3}{8\pi r_q^2} \right]^3 32\pi \sum_n \frac{\left| \int_0^\infty dr \left[\frac{3r^2}{8r_q^2} \right] e^{-(3r^2/8r_q^2)} u_{n,1}(r) \right|^2}{E_n}, \quad (10)$$

with $u_{n,l}$ the usual radial wave function and γ_0^{vac} a constant whose relationship to γ_0 will be discussed below. Performing the sum in (10) presents no difficulties. We find $\Delta E_{\text{vac}}(\gamma_0^{\text{vac}})^{-2}$ (in GeV^4) for $m_q = 0.33$ GeV, 0.55 GeV, 1.8 GeV, and 5.2 GeV is -0.0020 , -0.0022 , -0.0012 , and -0.00044 , respectively (-0.0040 , -0.0048 , -0.0032 , and -0.0012 , respectively), for $r_q = 0.30$ fm (0.25 fm). Most of the shift comes from values of $n \lesssim 4$. Now consider the effects of vacuum bubbling on our mesonic state. Far from the cigar-shaped region, the vacuum is unaffected by the presence of the "meson." However, near the string, the strong-coupling limit suggests that pair creation will be suppressed. As a simple model we take the vacuum bubbling to be excluded from a volume $V = \frac{4}{3}\pi b^{-3/2} + (\pi/b)r$, the volume of the cigar-shaped region shown in Fig. 5 corresponding to the e^{-1} contour. Note that although the coefficient of r is very uncertain, linearity (up to logarithms) is expected in the string picture⁴ so that the effect of ΔE_{vac} is bound to be absorbable into Δb . With these assumptions the observable shift in the energy of our mesonic system is

$$\Delta E(r) = \Delta E_{\text{sb}}(r) - \Delta E_{\text{cas}}(r), \quad (11)$$

where $\Delta E_{\text{cas}}(r) \equiv V \Delta \mathcal{E}_{\text{vac}}(r)$ is the Casimir shift due to the exclusion of vacuum bubbling.

Since our calculations of ΔE_{sb} are based upon the phenomenological strength γ_0 of meson decay amplitudes, they are reliable (within the substantial uncertainties indicated by the differences between Tables I and II). However, we have no such phenomenological constraint on

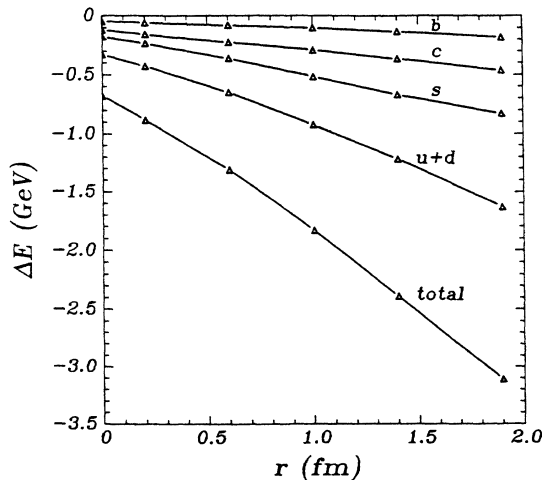


FIG. 6. $\Delta E(r)$ for $r_q = 0.3$ fm and $\gamma_0^{\text{vac}} = \gamma_0$. In addition to the total shift we show the contributions from each virtual-quark flavor individually.

γ_0^{vac} , and as a result, we know of no way of reliably estimating ΔE_{cas} . We therefore consider two rather extreme possibilities. In the first case one could take $\gamma_0^{\text{vac}} = 9\gamma_0$, as it will be in extreme strong coupling. We consider this to be unlikely since, as mentioned earlier, H_{sb} acts in the transition region between strong and weak coupling so that not only Fig. 3(b), but also Fig. 3(c) (in concert with gluonic fluctuations due to $\text{Tr}[2 - (U_1 U_2 U_3 U_4 + \text{H.c.})]$) contribute. In the extreme case of this type, we would have $\gamma_0^{\text{vac}} = \gamma_0$. For a very rough illustration of the magnitude and characteristics of $\Delta E(r)$, we adopt the latter relation and graph the results in Fig. 6. (Note that when, in the next section, we calculate a difference between two energy shifts, ΔE_{cas} will cancel out to allow us to draw more definite conclusions.)

Figure 6 shows that ΔE is a very nearly linear function of r , especially for $r \gtrsim 0.5$ fm. As mentioned above, this linearity is expected for ΔE_{cas} , but not obvious for ΔE_{sb} . Although a string model cannot be expected to be accurate for values of r much smaller than this, we note that the deviations from linearity in Fig. 6 are such as to produce an additional effective attractive potential at short distances which might be confused with the perturbative Coulomb-type potential in phenomenological fits to quarkonium spectroscopy.⁸

These results nevertheless suggest (independent of the uncertainties inherent in ΔE_{cas}) that the main effect of virtual pairs might be to merely renormalize the string tension. However, the magnitude of this renormalization is very large: Δb is of the same order of magnitude as the physical string tension. In the next section we will present a calculation which strongly suggests that it is unlikely that this very large shift can be absorbed as a renormalization of b with no state-dependent residual effects.

IV. SPIN-DEPENDENT ENERGY SHIFT

Let us now add spin-dependent forces into our model, and calculate the differential energy shift between two different mesonic systems, namely, a static spin-triplet $Q\bar{Q}$ pair and a static spin-singlet $Q\bar{Q}$ pair. Once again, our starting point is Eq. (1), but this time we must keep track of the quark spins. The expression (6) for the effective pair-creation operator implies that the matrix element in (1) is

$$2(s_c \chi_{s_b}^\dagger \sigma \chi_{-s_c}) \cdot \mathbf{I},$$

where the χ 's are Pauli spinors and

$$\mathbf{I} \equiv \left[\frac{3}{8\pi r_q^2} \right]^{3/2} \int d^3u d^3v e^{-(3u^2/8r_q^2)} \gamma_{00}^0(\mathbf{v}) \psi_b^*(\mathbf{v} + \frac{1}{2}\mathbf{u} + \frac{1}{2}r\hat{\mathbf{z}}) (\vec{\nabla}_c - \vec{\nabla}_b) \psi_c^*(\mathbf{v} - \frac{1}{2}\mathbf{u} - \frac{1}{2}r\hat{\mathbf{z}}) \quad (12)$$

is a spin-independent spatial overlap. If the $Q\bar{Q}$ pair is taken to be in a spin-singlet state, then we find the following expression for the energy shift from string breaking:

$$\Delta E_{\text{sb}}^{S=0}(r) = \sum_{\substack{n_b l_b m_b \\ n_c l_c m_c}} \left[\frac{\frac{1}{4}(|I_+|^2 + |I_-|^2 + 2|I_z|^2)}{V^0(r) - E_{bc}^{10}} + \frac{\frac{1}{4}(|I_+|^2 + |I_-|^2 + 2|I_z|^2)}{V^0(r) - E_{bc}^{01}} + \frac{\frac{1}{2}(|I_+|^2 + |I_-|^2 + 2|I_z|^2)}{V^0(r) - E_{bc}^{11}} \right], \quad (13a)$$

whereas for a spin-triplet $Q\bar{Q}$ pair (with $S_z=0$ for definiteness) we find

$$\Delta E_{\text{sb}}^{S=1}(r) = \sum_{\substack{n_b l_b m_b \\ n_c l_c m_c}} \left[\frac{\frac{1}{2}|I_z|^2}{V^0(r) - E_{bc}^{00}} + \frac{\frac{1}{4}(|I_+|^2 + |I_-|^2)}{V^0(r) - E_{bc}^{10}} + \frac{\frac{1}{4}(|I_+|^2 + |I_-|^2)}{V^0(r) - E_{bc}^{01}} + \frac{\frac{1}{2}(|I_+|^2 + |I_-|^2 + 3|I_z|^2)}{V^0(r) - E_{bc}^{11}} \right], \quad (13b)$$

where $I_{\pm} \equiv I_x \pm iI_y$, and in the energy denominators, $E_{bc}^{s_b s_c}$ is an abbreviation for $E_{n_b l_b, n_c l_c}^{s_b s_c}$. (s_b and s_c now denote the total spins of the intermediate mesons b and c , respectively.)

Vacuum corrections are the same for both $\Delta E_{\text{sb}}^{S=0}$ and $\Delta E_{\text{sb}}^{S=1}$, so by subtracting (13a) from (13b) we obtain a (in principle) physically measurable differential energy shift which is independent of the poorly known quantity γ_0^{vac} , and which cannot be absorbed into a redefinition of b . We find that

$$\Delta E_{\text{sb}}^{S=1}(r) - \Delta E_{\text{sb}}^{S=0}(r) \equiv \delta E(r) = \sum_{\substack{n_b l_b m_b \\ n_c l_c m_c}} \frac{1}{2} |I_z|^2 \left[\frac{1}{V^0(r) - E_{bc}^{00}} - \frac{1}{V^0(r) - E_{bc}^{10}} - \frac{1}{V^0(r) - E_{bc}^{01}} + \frac{1}{V^0(r) - E_{bc}^{11}} \right]. \quad (14)$$

In calculating δE we obtain the spin splittings from the usual meson hyperfine Hamiltonian,

$$H_{\text{hyp}} = \frac{32\pi}{9} \frac{\alpha_s}{m_1 m_2} \vec{S}_1 \cdot \vec{S}_2 \delta^3(\mathbf{r}), \quad (15)$$

taking

$$\frac{4}{3}\alpha_s = \begin{cases} 1.1 & \text{for } q = u, d, \text{ or } s, \\ 0.5 & \text{for } q = c \text{ or } b, \end{cases} \quad (16)$$

which values, in a potential model with $V = br + c - 4\alpha_s/3r$, give reasonable fits to the spin-averaged meson spectra, and in addition give the correct spin splittings in (14).

The spin-dependent potential between two light quarks can be obtained by performing our calculation for static quarks of mass 0.33 GeV. This corresponds to the usual assumption of the nonrelativistic quark model that the

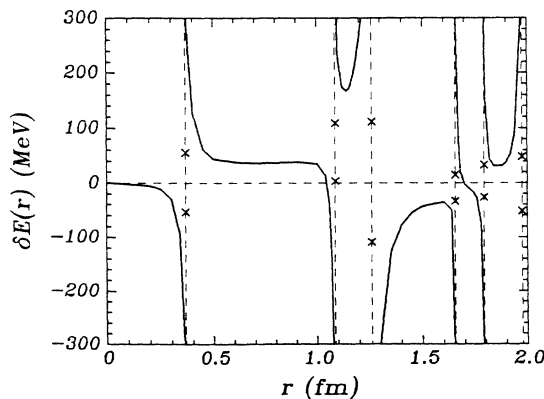


FIG. 7. $\delta E(r)$ from virtual $u\bar{u}$ and $d\bar{d}$ pairs, for $r_q = 0.30$ fm.

static potential is relevant to spectroscopy. This approximation could be spoiled by large relativistic corrections, but as an estimate of the energy shifts to be expected, and given the successes of the quark model, it is a reasonable one to make here. In Sec. V we will go beyond the static approximation to show that the estimates of this section are indeed qualitatively correct.

The $\delta E(r)$ produced by virtual $u\bar{u}$, $d\bar{d}$, and $s\bar{s}$ quarks is graphed in Figs. 7 and 8 for $r_q = 0.3$ fm. (The dependence on r_q is weak: δE changes by less than 20 MeV, over the whole range of r , when r_q is decreased from 0.3 to 0.25 fm.) The effects of the heavy quarks c and b cancel almost entirely in the difference (13b) and (13a); their combined contribution to $\delta E(r)$ is less than 1 MeV for all values of r . At the decay thresholds, the perturbative formula (14) diverges, so we must use degenerate perturbation theory, which, applied at these points, yields the results shown by X's on the graphs. Of course, it is only

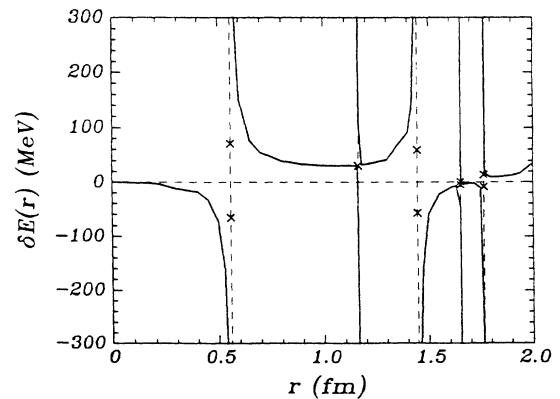


FIG. 8. $\delta E(r)$ from virtual $s\bar{s}$ pairs, for $r_q = 0.30$ fm.

away from these degeneracies that one can identify the eigenstate of the full Hamiltonian which is dominantly a perturbed string.

The only conclusion we wish to draw from these results is that the very large $\Delta E(r)$ of Fig. 6 has potentially large residual effects even after one redefines b . Figures 7 and 8 show that spin-dependent shifts of the order of 100 MeV are to be expected. In the next section we will verify this conclusion by considering the effects of nearby thresholds on the nucleon and ρ -meson masses.

V. APPLICATION TO THE N/ρ PROBLEM

The results of Sec. IV do not necessarily imply that the neglect of pair creation in ordinary (valence-) quark models will lead to substantial discrepancies with experiment: it is quite possible that pair-creation effects can be hidden in the handful of nonfundamental parameters that are characteristic of such models. It may be that only more fundamental calculations, such as Euclidean lattice QCD studies, will reveal the need for correctly incorporating virtual pairs. In fact, these calculations may already exhibit an example of such a need, namely, the so-called “ N/ρ problem” (the nucleon-to-rho mass ratio comes out too large). In this section we will see that a plausible explanation for this discrepancy may be found by examining the mass shifts produced by virtual decays of the ρ and N . In the preceding sections we have learned that the average effect of quark loops is simply to renormalize the string tension, but (see Figs. 7 and 8) that a state near a threshold can experience mass shifts which cannot be taken into account this way. In this section we therefore consider the effects on m_ρ and m_N of nearby thresholds.

In current lattice calculations that include virtual quark loops,¹ the masses m_q of the dynamical quarks are, out of computational necessity, taken to be rather large. They are so large, in fact, that the pion mass is greater than half the rho mass, making the ρ a stable particle. The “physical” ρ mass is obtained in such studies by smoothly extrapolating to $m_q \approx 0$ (where $m_\pi < \frac{1}{2}m_\rho$). We will argue that such a procedure will lead to an underestimate of m_ρ because the shift in m_ρ from its virtual decays to $\pi\pi$ is not a smooth function of m_π near $m_\pi = \frac{1}{2}m_\rho$. The shift may be calculated by computing the $\rho \rightarrow \pi\pi$ transition amplitude \mathcal{M} in the string-breaking model [the explicit formula for \mathcal{M} is obtained by multiplying Eq. (A1) of the Appendix by $\tilde{M}_\rho \tilde{M}_\pi^2$, where \tilde{M}_i is a normalization factor for meson i , as described in Ref. 3], and then using time-ordered perturbation theory (TOPT) to obtain

$$\Delta m_{\rho(\pi\pi)} = \frac{1}{(2\pi)^3 m_\rho} \int \frac{d^3k}{E_\pi^2} \frac{|\mathcal{M}|^2}{m_\rho - 2E_\pi}, \quad (17)$$

where \mathbf{k} is the momentum of one of the intermediate state pions. Recall that, in TOPT, virtual particles are on their mass shells, energy is not conserved at vertices, and each possible time ordering of a particular process is considered separately. The two time orderings for the $\rho \rightarrow \pi\pi$ self-energy loop are shown in Fig. 9. In the string-breaking model, it is reasonable to neglect the “Z” graph of Fig. 9(b), as the vertices there correspond to the

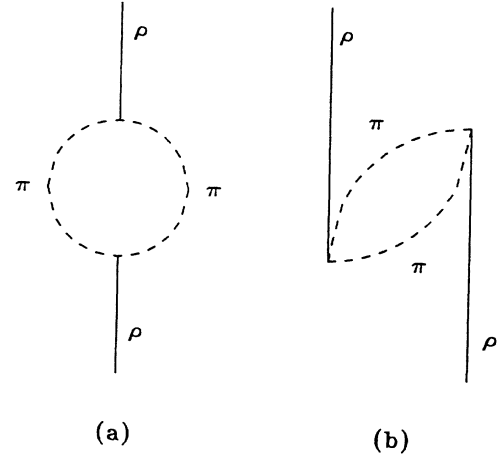


FIG. 9. The two time orderings for the $\rho \rightarrow \pi\pi$ self-energy loop.

creation and/or annihilation of three quark-antiquark pairs, a process which seems likely to be suppressed relative to the single pair-creation vertices of Fig. 9(a). (See Ref. 9 for a further discussion of this point). Neglecting the Z graph leads to expression (17).

In Fig. 10 we show $\Delta m_{\rho(\pi\pi)}$, as a function of the pion mass m_π , with the quark radius r_q taken to be 0.25 fm. (The results vary only by about 20% as r_q is varied between 0 and 0.3 fm.) There is an abrupt change in the mass shift as the ρ -decay threshold is crossed. Indeed, the second derivative of $\Delta m_{\rho(\pi\pi)}$ is discontinuous at this threshold. The dotted line in the figure shows how an extrapolation from large to small m_π could lead one to underestimate the ρ mass by approximately 70 MeV. (Un-

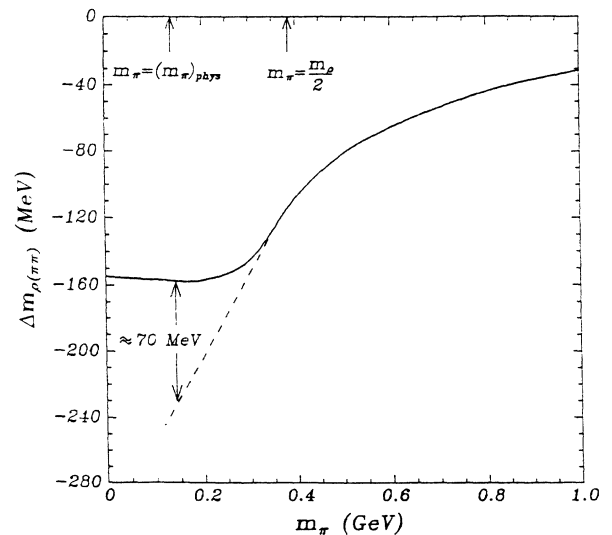


FIG. 10. The mass shift of the ρ from its virtual decays to $\pi\pi$. The dashed line shows how a smooth extrapolation from large to small m_π could be misleading. The physical pion mass and the threshold for ρ decay are indicated at the top of the graph.

quenched lattice calculations obtain $m_N/m_\rho \approx 1.6 \pm 0.2$, which corresponds to a 180 ± 90 -MeV underestimate of m_ρ .)

For comparison, the upper curve in Fig. 11 shows the results of a similar calculation of $\Delta m_{\rho(\omega\pi)}$, the mass shift that the ρ experiences from its virtual decays to $\omega\pi$. The curve is smooth, since no thresholds are crossed, indicating that virtual decays to this and higher-mass states cannot wash out the jump in $\Delta m_{\rho(\pi\pi)}$. This is of course consistent with our conclusion that the effects of high-mass states can be absorbed into the string tension. The lower curve in Fig. 11 shows $\Delta m_{N(N\pi)}$, the mass shift of the nucleon from $N \rightarrow N\pi$. Since the string-breaking model has not been fully studied for baryon decays we calculated $\Delta m_{N(N\pi)}$ using the pseudovector coupling

$$\mathcal{L}_{\text{int}} = \frac{g}{2m_N} \bar{N} \gamma_\mu \gamma_5 \vec{\tau} N \cdot \partial^\mu \vec{\pi}. \quad (18)$$

with coupling constant $g = 13.5$, and with a form factor $e^{-k^2/6\delta^2}$ to account for the finite size of the hadrons. This gives

$$\Delta m_{N(N\pi)} = \frac{3\pi g^2}{(2\pi)^3} \int \frac{dk}{E_\pi E_N (E_N + m_N)} \frac{k^4 e^{-k^2/6\delta^2}}{m_N - (E_N + E_\pi)}. \quad (19)$$

Fits to baryon spectra and baryon decay rates¹⁰ give $\delta \approx 0.3$ to 0.4 GeV. The results of Fig. 11 were obtained with $\delta = 0.3$ GeV. Although the magnitude of $\Delta m_{N(N\pi)}$ is naturally quite sensitive to δ , the shape of the curve is not, and we are mainly interested in showing that, in the ratio m_N/m_ρ , the jump in m_ρ is not canceled out by a corresponding jump in m_N . We also checked that the pseudoscalar coupling $\mathcal{L}_{\text{int}} = g \bar{N} \gamma_5 \vec{\tau} N \cdot \vec{\pi}$ produces a similarly smooth nucleon mass shift. As with m_ρ , it is unnecessary to consider higher-mass states since their effects can be subsumed into the string tension b .

These results strongly suggest that the N/ρ problem is at least partially a result of the apparently invalid procedure of smoothly extrapolating m_N/m_ρ through the threshold for ρ decay, and that lattice calculations of m_N/m_ρ will become accurate only when they are performed with m_π near its physical value.

VI. CONCLUSIONS

It seems likely that the model we have presented here of quark pair creation in mesons is at least qualitatively correct: in addition to being in accord with strong-coupling QCD, it has a demonstrated ability to successfully describe strong meson decays. The main conclusions we have drawn from the model are as follows.

(i) Virtual pair creation in mesonic systems leads to a very large energy shift. (This is not unexpected, for the energy shift from each nearby virtual decay mode ought to be roughly the size of a typical strong decay width, i.e.,

$$M(A \rightarrow BC) = \left[\frac{3}{8\pi r_q^2} \right]^{3/2} \int d^3r d^3u d^3y \gamma_{00}^0(\mathbf{r}, \mathbf{y}) e^{-(3u^2/8r_q^2)} \times \psi_b^*(\frac{1}{2}\mathbf{r} + \frac{1}{2}\mathbf{u} + \mathbf{y}) \psi_c^*(\frac{1}{2}\mathbf{r} + \frac{1}{2}\mathbf{u} - \mathbf{y}) \vec{\alpha} \cdot (i\vec{\nabla}_b + i\vec{\nabla}_c + \mathbf{q}) \psi_a(\mathbf{r}) e^{i\mathbf{q} \cdot (\mathbf{r} + \mathbf{u})/2}, \quad (A1)$$

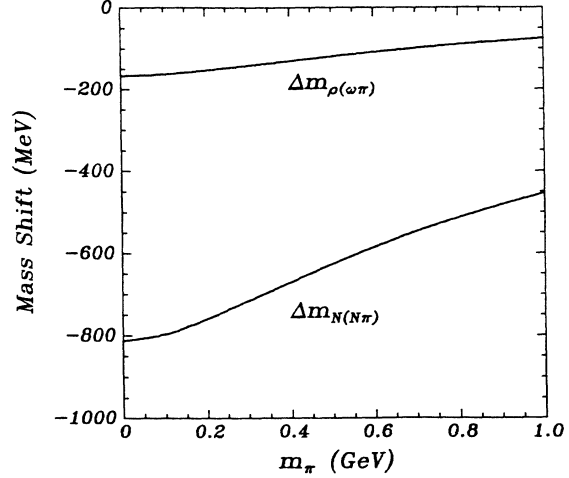


FIG. 11. The ρ mass shift from $\rho \rightarrow \omega\pi$ (upper curve), and the nucleon mass shift from $N \rightarrow N\pi$ (lower curve).

about 100 MeV.) For the case of static $Q\bar{Q}$ sources, the shift is an almost linear function of the distance between the sources; hence, it mainly serves just to renormalize the string tension b .

(ii) The virtual pairs will, nevertheless, make their presence felt in spectroscopy with a strength of the order of 100 MeV, due to spin-dependent and/or nearby-threshold effects, which are not the same for all mesons and so cannot be absorbed by a single shift in b .

Thus, any *fundamental* calculation of the hadron spectrum which hopes to be accurate to better than about 100 MeV must correctly treat pair-creation effects. We have indicated how the N/ρ problem of lattice QCD may be ascribed to a failure to do so.

ACKNOWLEDGMENTS

This work was supported in part by a grant from the Natural Sciences and Engineering Research Council of Canada.

APPENDIX

The numerical values of γ_0 (the string-breaking amplitude) and r_q (the constituent quark radius) that we used in our calculations of ΔE were obtained by fitting to meson decay data. Specifically, our fitting procedure was as follows. We calculated meson decay amplitudes in the string-breaking model of Ref. 3, replacing their effective pair-creation operator C_r [see Eq. (4)] by the smeared pair-creation operator \bar{C}_r defined in Eq. (6). The expression that we thereby obtained for the amplitude for the decay process $A \rightarrow BC$ is

TABLE III. The decays used in the goodness-of-fit test. Also shown are two sample sets of calculated decay amplitudes, for $r_q=0$ and $r_q=0.3$ fm, and the experimental amplitudes. [The latter are taken from the Particle Data Group (Ref. 11).] Note that we have, in all cases, ignored the phases of the amplitudes, as they are irrelevant to our fitting procedure.

Decay	Calculated amplitudes ($\sqrt{\text{MeV}}$)		Experimental amplitude ($\sqrt{\text{MeV}}$)
	$r_q=0$	$r_q=0.3$ fm	
<i>D waves</i>			
$a_2(1320) \rightarrow \rho\pi$	6.7	5.7	8.8 ± 0.3
$a_2(1320) \rightarrow \eta\pi$	4.9	4.1	4.0 ± 0.1
$a_2(1320) \rightarrow K\bar{K}$	3.4	2.9	2.3 ± 0.1
$f_2(1270) \rightarrow \pi\pi$	11.0	9.1	12 ± 1
$f_2(1270) \rightarrow K\bar{K}$	3.1	2.6	2.3 ± 0.2
$f_2(1270) \rightarrow \eta\eta$	1.0	0.86	1.0 ± 0.2
$f_2'(1525) \rightarrow \pi\pi$	0.90	0.72	0.8 ± 0.4
$K_2^*(1430) \rightarrow K\pi$	7.8	6.4	6.7 ± 0.5
$K_2^*(1430) \rightarrow K^*\pi$	4.1	3.5	5.0 ± 0.5
$K_2^*(1430) \rightarrow \rho K$	3.3	2.8	3.0 ± 0.4
$K_2^*(1430) \rightarrow \omega K$	1.3	1.1	2.0 ± 0.4
$K_2^*(1430) \rightarrow K\eta$	0.8	0.67	2.2 ± 0.7
$K_1(1280) \rightarrow K^*\pi$	2.7	2.3	2.6 ± 0.5
$K_1(1400) \rightarrow K^*\pi$	1.1	0.94	2.6 ± 0.9
$b_1(1230) \rightarrow \omega\pi$	2.4	2.1	3.6 ± 0.5
<i>F waves</i>			
$\rho_3(1690) \rightarrow \pi\pi$	6.4	4.3	6.9 ± 0.6
$\rho_3(1690) \rightarrow \omega\pi$	3.8	2.7	5.6 ± 1.6
$\rho_3(1690) \rightarrow K\bar{K}$	3.2	2.2	1.7 ± 0.3
$\omega_3(1670) \rightarrow \rho\pi$	6.2	4.4	8 ± 2
$\phi_3(1850) \rightarrow K\bar{K}$	5.8	4.0	7 ± 2
$\phi_3(1850) \rightarrow K^*\bar{K}$	3.1	2.2	5 ± 2
$K_3^*(1780) \rightarrow K\pi$	5.7	3.9	4.9 ± 1.0
<i>G waves</i>			
$f_4(2030) \rightarrow \pi\pi$	5.2	2.9	6 ± 1
$f_4(2030) \rightarrow K\bar{K}$	2.3	1.3	1.3 ± 0.4
$f_4(2030) \rightarrow \eta\eta$	1.0	0.58	0.45 ± 0.23
$K_4^*(2060) \rightarrow K\pi$	3.4	1.9	4 ± 1

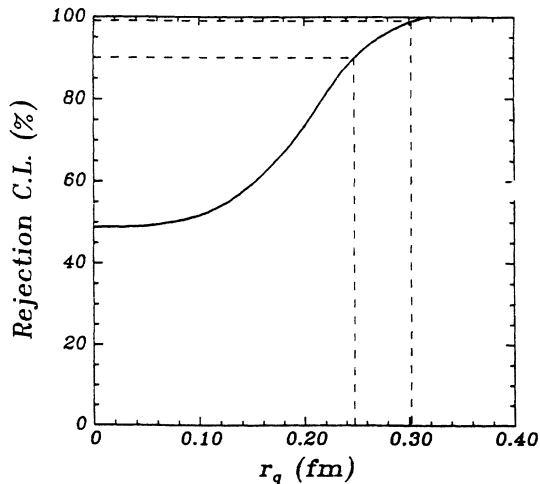


FIG. 12. Goodness of fit vs r_q . The dashed lines show the 90% and 99% levels, which correspond to r_q values of 0.25 fm and 0.30 fm, respectively.

where \mathbf{q} is the momentum of B . This expression reduces, as it should, to Eq. (6) of Ref. 3 when $r_q \rightarrow 0$. We also used the same wave functions as in Ref. 3, namely, harmonic-oscillator wave functions, with oscillator parameter $\beta = 0.4 \text{ GeV}$ [β is defined by $\psi(\mathbf{r}) \sim (\text{polynomial}) \times e^{-\beta^2 r^2/2}$], and the same phase-space factors as well, so that from (A1) we could directly calculate decay amplitudes as functions of r_q and γ_0 .

For each of a series of values of r_q , we fitted γ_0 to the decay $\rho \rightarrow \pi\pi$, and then calculated the rates for the decays shown in Table III. We chose to look at decays with high orbital angular momentum in the final state, as there is a good deal of data available for them, and they are quite sensitive to a softening of the pair-creation operator (i.e., to an increase in r_q). The goodness of fit to the 26 decays of Table III is shown, as a function of r_q , in Fig. 12. We can read off that r_q is less than 0.3 fm at the 99% confidence level, and less than 0.25 fm at the 90% confidence level. These are the values we quoted in the text. The values of γ_0 corresponding to these r_q 's are

0.77 and 0.72, respectively.

The goodness-of-fit calculations require, of course, a value for the theoretical error σ_t of our calculated decay amplitudes. We “measured” σ_t to be 27% when $r_q=0$ (which, as Fig. 12 shows, is the value slightly preferred by

the data), and we used this value for all of our calculations. We checked, however, that our results are not very sensitive to changes in σ_t . For example, even if σ_t is allowed to be as large as 40%, one can still conclude that $r_q < 0.3$ fm, with a confidence level of 85%.

¹Unquenched lattice calculations are reviewed, and an extensive list of references is given in A. Ukawa, Nucl. Phys. B (Proc. Suppl.) **10A**, 66 (1989). See also Stephen Sharpe in *Glueballs, Hybrids, and Exotic Hadrons*, edited by Suh-Urk Chung (AIP Conf. Proc. No. 185) (AIP, New York, 1989), p. 55. In addition, for unquenched calculations of the heavy-quark potential, see M. P. Grady, D. K. Sinclair, and J. B. Kogut, Phys. Lett. B **200**, 149 (1988); M. Faber *et al.*, Helv. Phys. Acta **60**, 717 (1987); P. de Forcrand, Nucl. Phys. A**461**, 361c (1987); E. Laermann *et al.*, Phys. Lett. B **173**, 437 (1986).

²See, for example, E. C. Poggio and H. J. Schnitzer, Phys. Rev. D **19**, 1557 (1979); M. G. Olsson and C. J. Suchyta III, Phys. Rev. Lett. **57**, 37 (1986); N. A. Törnqvist, Acta Phys. Pol. **B16**, 503 (1985); W. S. Jaronski and D. Robson, Phys. Rev. D **32**, 1198 (1985); Y. Nogami and N. Ohtsuka *ibid.* **26**, 261 (1982); M. Brack and R. K. Bhaduri, *ibid.* **35**, 3451 (1987); N. Barik and S. N. Jena, *ibid.* **22**, 1704 (1980).

³R. Kokoski and N. Isgur, Phys. Rev. D **35**, 907 (1987).

⁴N. Isgur and J. Paton, Phys. Rev. D **31**, 2910 (1985).

⁵J. Kogut and L. Susskind, Phys. Rev. D **11**, 395 (1975).

⁶By different “topologies” we mean configurations which cannot be continuously transformed into one another.

⁷See S. Godfrey and N. Isgur, Phys. Rev. D **32**, 189 (1985); S. Capstick and N. Isgur, *ibid.* **34**, 2809 (1986), and references therein.

⁸For a discussion of this point, see Olsson and Suchyta (Ref. 2).

⁹N. Isgur, C. Morningstar, and C. Reader, Phys. Rev. D **39**, 1357 (1989).

¹⁰See, for example, L. A. Copley, G. Karl, and E. Obryk, Nucl. Phys. **B13**, 303 (1969); R. Koniuk and N. Isgur, Phys. Rev. D **21**, 1868 (1980). These authors find $\beta=0.4$ GeV, but do not consider the structure of the pion which will soften the form factors.

¹¹Particle Data Group, M. Aguilar-Benitez *et al.*, Phys. Lett. **170B**, 1 (1986).